J Clin Monit Comput (2018) 32:729–740
DOI 10.1007/s10877-017-0060-9

ORIGINAL RESEARCH

K-band Doppler radar for contact-less overnight sleep marker assessment: a pilot validation study

Rakesh Vasireddy[1,3] · Corinne Roth[2] · Johannes Mathis[2] · Josef Goette[3] · Marcel Jacomet[3] · Andreas Vogt[1]

Received: 3 June 2017 / Accepted: 28 August 2017 / Published online: 11 September 2017

Abstract An estimated 45 million persons in Europe are annually subjected to sleep-wake disorders. State-of-the-art polysomnography provides sophisticated insights into sleep (patho)physiology. A drawback of the method, however, is the obtrusive setting dependent on a clinical-based sleep laboratory with high operational costs. A contact-less prototype was developed to monitor limb movements and vital signs during sleep. A dual channel K-band Doppler radar transceiver captured limb movements and periodic chest wall motion due to respiration and heart activity. A wavelet transform based multi-resolution analysis (MRA) approach isolated limb movements, respiration, and heart rate from the demodulated signal. A test bench setup characterized the prototype simulating near physiological chest wall motions caused by periodic respiration and heartbeats in humans. Single- and multi-tone test bench simulations showed extremely low relative percentage errors of the prototype for respiratory and heart rate within −2 and 1%. The performance of the prototype was validated in overnight comparative studies, involving two healthy volunteers, with polysomnography as the reference. The prototype has successfully classified limb movements, with a sensitivity and specificity of 88.9 and 76.8% respectively, and has achieved accurate respiratory and heart rate measurement performance with overall absolute errors of 1 breath per minute for respiration and 3 beats per minute for heart rate. This pilot study shows that K-band Doppler radar and wavelet transform MRA seem to be valid for overnight sleep marker assessment. The contact-less approach might offer a promising solution for home-based sleep monitoring and assessment.

Keywords Sleep-wake disorders · Contact-less · Doppler radar · Wavelet transform · Monitoring

1 Introduction

Sleep is an important pillar of well-being, and sleep quality is associated with short and long-term effects on health. An estimated 45 million persons in Europe [1] are annually subjected to sleep-wake disorders. Insomnia, prevalent in 10–15% of the general population [2], is associated with significant depression morbidity and anxiety [3]. Sleep-disordered breathing (SDB), prevalent among 10–17% (men) and 3–9% (women) of the general population [4], is identified as one of the leading causes of hypertension and cardiovascular morbidity [5], postoperative delirium [6], and well recognized as a major cause of work- and driving accidents [7]. Despite their high prevalence rates today and significant projections for the future [8], sleep-wake disorders remain largely under-diagnosed and inadequately treated [9, 10]. The current standard for the diagnosis of

A brief summary of this work was presented at the European Medical and Biological Engineering Conference (EMBEC) 13/06/17 in Tampere, Finland. The abstract was also presented at the annual meeting of Swiss Society for Sleep Research, Sleep Medicine and Chronobiology (SSSSC) 11/05/17 in Lugano, Switzerland.

✉ Andreas Vogt
Andreas.Vogt@insel.ch

[1] Department of Anaesthesiology & Pain Medicine, Inselspital, Bern University Hospital, University of Bern, Bern, Switzerland

[2] Sleep-Wake-Epilepsy-Centre, Department of Neurology, Inselspital, Bern University Hospital, University of Bern, Bern, Switzerland

[3] Institute for Human Centered Engineering, HuCE-microLab, Bern University of Applied Sciences, Bern, Switzerland

sleep-wake disorders is overnight attended polysomnography (PSG) [11].

Polysomnography the current state-of-the-art diagnostic tool provides sophisticated insights into sleep physiology and mechanisms of sleep-wake disorders. A drawback of the method, however, is an obtrusive patient setting dependent on a clinical-based sleep laboratory with high operational costs. Single-night polysomnography is often criticized for not being an accurate representative sample of a patient's sleep due to its first-night effect and night-to-night variability [12–14].

In conjunction with full scale single-night PSG studies, sleep diaries/logs [15] are often used to record subjective reports of sleep-wake behaviors and to evaluate the severity of chronic sleep-wake disorders such as insomnia, delayed sleep phase syndrome (DSPS), SDB, and fragmented sleep. Although subjective reports enable estimation of overall sleep-wake behaviors, studies have shown that these self-reports have severe limitations leading to under/over-estimation of total sleep time, sleep on-sets and wake [16, 17].

Recent developments in micro-technology have enabled non-invasive ambulatory activity monitory and sleep-wake behaviors. Actigraphy [18] uses sensitive, body worn, accelerometers to measure the movements of the patients during sleep and to derive objective sleep quality parameters. Although Actigraphy mitigates the problem of under/over-estimation due to subjective perceptions of sleep, the physiological information that can be obtained from these recordings are very much limited due to its dependency on movements of the patient for sleep-wake classification. Hence, Actigraphy is often inappropriate for clinical diagnosis and long term monitoring [19].

Overnight variations in cardiorespiratory features during sleep have been extensively researched and show established characteristic variations in association with sleep stages [20, 21]. Heart rate variability (HRV) calculated from Electrocardiogram (ECG) and respiratory effort from respiratory inductance plethysmography have been used to classify sleep stages [22], and even to screen sleep-wake disorders such as sleep apnea [23]. Although ECG and respiratory inductance plethysmography allow patients to monitor sleep from the comfort of their homes, these techniques are significantly obtrusive since the patient will have to wear the apparatus for an average of 8 h each night.

Recent developments in wireless technology have enabled contact-less acquisition of physiological signals. Doppler radar technology [24], based on the scattering of continuous wave radiation, was first introduced by Lin [25] measuring periodic chest wall motion due to respiration in animals as well as humans. Recent studies have demonstrated contact-less measurement of respiration and heart rate [26, 27]. In these studies, the participants are seated in front of the Doppler radar with little or no movements. A single measurement period ranges between a few seconds to a few minutes. Such a setup differs from a real-life sleeping subject under measurement as follows: (i) the subject exhibits a wider range of motions, positions, and orientations relative to a stationary Doppler radar apparatus, (ii) the cardio-pulmonary parameters being measured are subjected to a greater range of variations due to over-night circadian changes and longer measurement periods up to eight hours.

Studies validating Doppler radar with reference to the current gold-standard PSG are very much essential in order to fully evaluate the true potential of the technology in assessing overnight cardio-pulmonary variations, and to establish its implications in sleep-wake disorder diagnosis.

This work aims to:

1. present the hardware and signal processing methods of a miniaturized K-band Doppler radar prototype for limb movements, respiratory and cardiac monitoring.
2. evaluate the measurement of respiratory and cardiac parameters using a test bench for near physiological simulations.
3. validate the developed prototype for the assessment of limb movements, as well as respiratory and heart rate against the gold standard PSG in two overnight healthy volunteer studies.

2 Materials and methods

2.1 Principle of operation

During sleep, various internal organs subject the human body to movements ranging from a few micrometers to several centimeters. The main sources of these movements are: (i) skeletal muscle contractions and relaxations, (ii) respiration, (iii) heartbeats, and (iv) blood perfusion through capillary network. Limb movements during sleep due to skeletal muscle contractions and relaxations routinely lie in the frequencies of 2.5–4 Hz. Respiration due to inhalation and exhalation involves small periodic motion (0.1–0.4 Hz) of the chest wall and abdomen in the range of 1–5 mm. Similarly, volumetric changes of the heart during its beats result in pulsations of the chest wall causing surface level periodic (0.7–2 Hz) displacements in the range of 0.5–1 mm. Blood perfusion through the capillary network due to arterial pulsations induce displacements at the skin surface in the range of 0.01–0.06 mm, and often correlate highly with heart rate.

Doppler radar technology can be used to measure limb movements as well as periodic surface level displacements due to respiration, heartbeats, and blood perfusion. K-band Doppler radar transceiver was used to measure limb movements, respiration, and heartbeats in this study. Although studies have demonstrated contact-less blood perfusion and

pressure measurement using Doppler radar [28], this was deemed in-essential for this study to achieve the overall goal of over-night cardiopulmonary monitoring for sleep-wake assessment.

An electromagnetic wave *T(t)* transmitted (Fig. 1) by the Doppler radar towards the subject's chest wall can be mathematically represented as:

$$T(t) = \cos(2\pi ft) \tag{1}$$

where t is time and f is the frequency of operation. A significant component of *T(t)* gets reflected at the air-skin interface. This reflected wave *R(t)* can be represented as:

$$R(t) = A\cos\left(2\pi ft + 2\pi f/c(2d_0 + 2d(t))\right) \tag{2}$$

where d_0 is the static distance between the Radar transceiver and the subject's chest wall, *d(t)* is the periodic chest wall displacement in time t, and c is the speed of electromagnetic waves in air (3×10^8 m/s). The scalar A represents the amplitude change and will be a fraction of the transmitted wave. Equation 2 shows that the static distance and the periodic chest wall motion (mainly caused by respiration and heart rate) are contained in the phase component of the received wave and can be recovered using appropriate demodulation and signal processing techniques.

2.2 Hardware design

2.2.1 Transceiver

We used a dual channel Doppler radar transceiver (K-LC5, RFBeam GmbH, Switzerland) in combination with a custom designed data acquisition system described in detail at the end of this section. The K-LC5 transceiver is a quadrature transceiver operating at 24 GHz with a built-in mixer stage to remove components that are common to the transmitted and received waves. The transceiver outputs only the phase components of the received wave, which hold the static distance, limb movements respiratory as well as heart rate information, as a pair of orthonormal signals that are commonly referred to as baseband signals or intermediate frequencies. Quadrature transceivers compensate for the null point problem and are proven to be more reliable in comparison to single channel transceivers for small amplitude measurements [29]. The orthonormal baseband signal pair, I(t) and Q(t), after the in-built mixer stage can be mathematically represented as:

$$I(t) = A_1\cos\left(2\pi f/c(2d_0 + 2d(t)\right) \tag{3}$$

$$Q(t) = A_2\cos\left(2\pi f/c(2d_0 + 2d(t) + \pi/2\right) \tag{4}$$

2.2.2 Data acquisition

The baseband signals from the transceiver are amplified prior to digitization, using two low-noise, non-inverting amplifiers with a gain of 16. Two 12-bit synchronously sampling analog to digital converters digitize the amplified signals at a sampling rate of 500 Hz. A 32-bit ARM Cortex-M4 processor (MK20DX256VLH7, NXP Semiconductors, USA) package the digitized samples further. The time-stamped packets were logged onto a SD-card for off-line analysis.

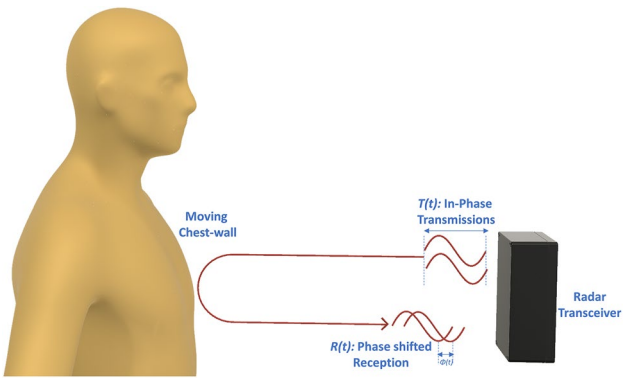

Fig. 1 Doppler radar based cardiopulmonary monitoring; principle of operation. Reflections of in-phase transmissions T(t), from the moving chest wall due to periodic respiratory and cardiac activity, give rise to phase shifted receptions *R*(*t*)

2.3 Signal processing

2.3.1 Demodulation

Accurate estimation of *d(t)* involves efficient combining of *I(t)* and *Q(t)* to determine the phase of the reflected wave. Several schemes have been proposed for this purpose [26, 27, 30], the method of Arc Tangent being the most commonly used. The arctangent demodulation is also called "nonlinear demodulation" or "direct phase demodulation" in the literature and can be mathematically represented as:

$$\emptyset(t) = \arctan\left(Q(t)/I(t)\right) \tag{5}$$

In order to efficiently apply the arc-tangent demodulation scheme on the baseband signals, the static distance d_0 existing as a direct current (DC) component in the baseband signals must be estimated and eliminated as it acts as a linear transform on the I and Q components, resulting in erroneous phase estimates [27].

The center of the arc formed in the IQ-plot eliminates the DC component. The iterative Levenberg–Marquardt center estimation algorithm, with the initialization parameters provided by the algebraic Taubin fit method, was found to be the most accurate for this purpose [31]. Figure 2 shows the arc formed by the sample I and Q data points in the IQ-plot and the center estimation using Levenberg–Marquardt algorithm.

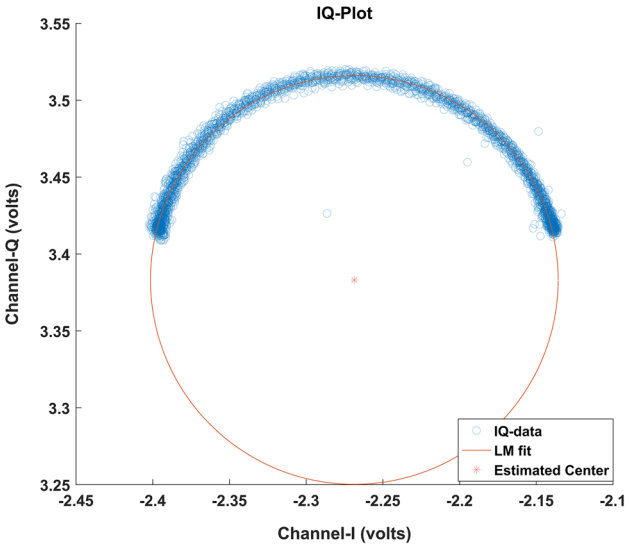

Fig. 2 Sample IQ-Plot with center estimation using Levenberg–Marquardt (LM) algorithm. The DC components of channels I and Q are eliminated by estimating the center of the arc using LM fit

2.3.2 Multiresolution analysis

Upon demodulation, the recovered phase signal $\phi(t)$ is a combination of limb movements, periodic chest wall motion due to respiration and heartbeats, and reflections from other undesirable random movements occurring within the vicinity of measurement. In order to isolate individual physiological signal components from $\phi(t)$, an efficient signal separation and processing scheme is essential. Band-pass filters have been commonly used to isolate physiological signals [31] since the limb movements during sleep as well as the cardiopulmonary signals exist in well-defined frequency bands. Although such filters can be used for rudimentary separations, accurate reconstruction of respiration and heart rate is challenging, as the process of filtering often results in signal distortion, amplitude modulation of the heart rate signal, and fails to solve the problem of higher order respiration harmonics falling within the frequency region of the heart rate [32].

Wavelet transform (WT) is a relatively new mathematical tool and since its introduction in 1909, WT has been successfully applied in a wide range of fields like data compression, numerical analysis, signal and image processing, and finance. The WT of a signal f can be mathematically represented as:

$$W_s f(a) = 1/\sqrt{s} \int_{-\infty}^{+\infty} f(t)\psi\left(\frac{t-a}{s}\right)dt \tag{6}$$

where s and a are the scale and translation factors of the mother wavelet ψ function, the linear combination of whose dilations and translations represent the signal $f(t)$ [33]. Mallat [34] proposed first the concept of multiresolution analysis (MRA) i.e. multi-level decomposition of a discretely sampled signal. In MRA, for a discrete signal $f(t)$ sampled at a regular interval, the s and a factors are discretized as: $s=2^j$, $a=2^j k$, and the wavelet function is expressed as:

$$\psi_{j,k}(t) = 2^{-\frac{j}{2}}\psi\left(2^{-j}t-k\right), \quad j, \quad k \in Z \tag{7}$$

where Z is the integral set. MRA enables examination of the signal at dyadic frequency bands with varying resolutions by decomposing the signal into approximate (CA) and detailed coefficients (CD). At a given decomposition level n, CA_n contains frequencies from 0 to $fs/2^n$ and CD_n contains frequencies between $fs/2^n$ to $fs/2^{n+1}$, where fs is the sampling rate of the signal $f(t)$ being decomposed.

The demodulated signal $\emptyset(t)$, with a sampling frequency of 50 Hz, was analyzed by using a 5-level MRA decomposition as described above. Figure 3 illustrates in detail the 5-level MRA scheme and the frequency bands of CAs and CDs at each level. Upon wavelet decomposition, CD_4 was reconstructed to estimate limb movements. Similarly, CA_5 and CD_5 were reconstructed to estimate respiration rates between 6 and 26 breaths per minute and heart rates between 46 and 92 beats per minute.

2.4 Test bench

A test bench setup was used to simulate the physiological motion of a human chest wall in order to characterize the response of the developed prototype. The setup comprised of a surface (plate), with a reflection coefficient and radar cross-section area close to that of a human thorax and a vibration exciter (Type 4809, Brüel & Kjaer, Denmark). This linear system converts electrical signals into mechanical vibrations. An arbitrary waveform generator (33220A, Keysight Technologies, USA) was programmed to generate single-tone (one frequency) and multi-tone (a combination of two or more frequencies) vibrations, simulating the physiological motion of a human chest wall with 8–24 breaths per minute and heart rates of 40–100 beats per minute. A power amplifier (Type BAA 120 TIRA, BEAK Electronic Engineering GmbH, Germany) amplified the waveforms before they were fed to the vibration exciter. Figure 4 shows the surface, the vibration exciter, and the relative position of the prototype with reference to the test bench setup.

$$A_{var}\sin\left(2\pi f_{var}\right) \tag{8}$$

$$A_{1var}\sin\left(2\pi f_{1var}\right) + A_{2var}\sin\left(2\pi f_{2var}\right) \tag{9}$$

Equation 8 represents the general form of single-tone waveforms generated, where A_{var} is the variable amplitude

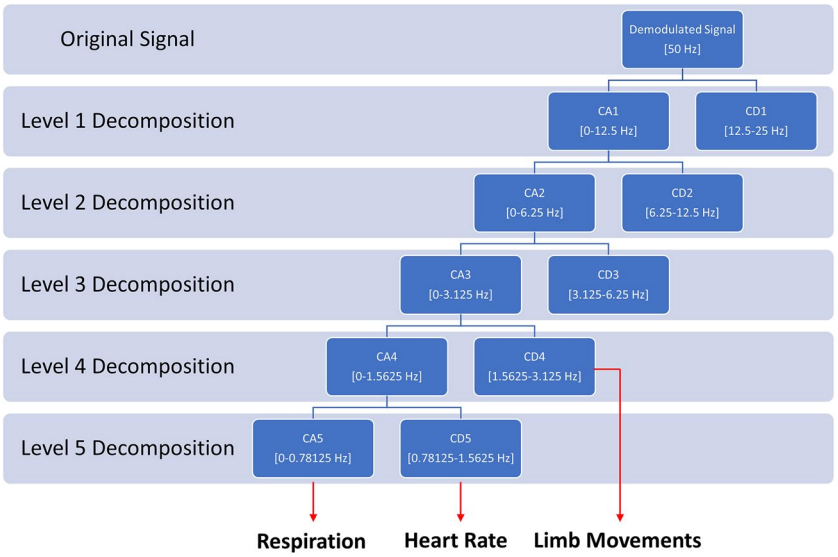

Fig. 3 Multiresolution analysis. Signal decomposition using dyadic frequency bands and extraction of physiological signals of interest. Limb movements are extracted from CD_4, while respiration and heart-rate waveforms are extracted from CA_5 and CD_5, respectively

Fig. 4 Test bench setup: exciter with the vibrating surface mounted on top (**a**) and the prototype positioned (**b**)

and f_{var} is the frequency parameters of the wave. Similarly, Eq. 9 represents the general form of multi-tone waveforms generated, where A_{1var} and f_{1var} are the variable amplitude and frequency parameters of the wave representing respiration (modelled as a sine wave), and A_{2var} and f_{2var} are the variable amplitude and frequency parameters of the wave representing chest wall movement due to periodic heartbeats (modelled as a sine wave as well).

2.5 Clinical validation

In January 2017 after obtaining informed consent two volunteers were assessed for limb movements, respiratory rate and heart rate in two overnight experiments simultaneously with the K-band Doppler radar prototype and the state-of-the-art reference method e.g. polysomnography at the Sleep-Wake-Epilepsy-Centre, Department of Neurology, Inselspital, Bern University Hospital. The perpendicular distance between the Doppler radar transceiver and the sternum was 40 cm at an angle of 0° to the chest wall of the volunteer. The volunteers were unrestrained during these overnight measurements, hence their relative positions and angles with respect to the prototype was never constant. The prototype used for these experiments was equipped with a flash card (microSD 32 GB, SanDisk, USA) for overnight data logging as well as for easy transfer to a personal computer for carrying out post hoc analysis The Embla Sleep Diagnostics system (Natus Medical Incorporated, USA) performed full polysomnography under the supervision of trained sleep technicians. The sampling rates of the polysomnography system were in accordance with the recommendations set by the American Academy of Sleep Medicine (AASM) [11]. Respiration was recorded by using nasal pressure sensor and thoracic and abdominal strain gages. Body movements were recorded by an accelerometer based position sensors, mounted on the thorax of the subject. A sleep epoch of 30 s was defined according to the AASM criteria. The polysomnography raw data was exported, as individual signals, in the European Data Format (EDF) for post hoc analysis.

2.6 Safety considerations

The Doppler radar transceiver of this study has maximum total output power of +19 dBm or 80 mW EIRP (Equivalent Isotropically Radiated Power), in-line with ubiquitous Wi-Fi router systems. When placed at a distance of 40 cm, the power density of the prototype is well below the recommendations set by Federal Communications Commission (FCC) and The European Telecommunications Standards Institute (ETSI). Hence, the prototype poses no health implications for long-term continuous monitoring.

2.7 Statistics

Data collection, data management, and signal processing were performed using MATLAB (R2016b, The MathWorks Inc., USA). MedCalc (version 17.5.5, MedCalc Software bvba, Belgium) was used for data analysis and plotting. For multi-tone test bench results, relative error percentages were calculated using the set and the measured variable values. A sensitivity–specificity analysis was used for limb movement agreement of both methods. Sensitivity was defined as the ratio of true positives (detected double-epochs with limb movements) to the sum of true positives and false negatives (total number of double-epochs with limb movements). Specificity was defined as the ration of true negatives (double-epochs with no limb movements) to the sum of true negatives and false positives (total number of double-epochs with no limb movements). Agreement of both methods for respiratory and heart rate was described by a detailed Bland–Altman [35, 36] analysis.

3 Results

3.1 Test bench

3.1.1 Single-tone measurements

Single-tone waveforms were used to characterize the response of the prototype, and its I and Q channels, with respect to varying distance, measured perpendicularly between the prototype and the surface of the vibration exciter. The vibration frequency f_{var} was set to 1 Hz, and the amplitude Avar was maintained at 0.5 mm, corresponding to physiological surface level displacements due to heart activity. The distance between the prototype and the setup was varied from 20 to 120 cm in incremental steps of 10. Table 1 shows the signal-to-noise ratio (SNR) of the channels I and Q, calculated relative to the carrier (dBc), as a function of varying distance. Figure 5 illustrates the following three important scenarios of Table 1. (i) Both channels are operating in regions distant from their null points (D = 40 cm), (ii) channel I is close to its optimum point and Q to its null point (D = 50 cm), and (iii) channel Q is approaching its optimum point and I its null point (D = 70 cm).

Table 1 Signal to noise ratio (SNR) results as a function of varying distance for channel I and Q expressed in dBc (power ratio of a signal to a carrier signal)

Distance (cm)	SNR—I (dBc)	SNR—Q (dBc)
20	30.604	24.218
30	26.177	26.211
40	21.280	27.764
50	25.511	5.133
60	13.359	18.959
70	−5.499	9.917
80	15.018	10.442
90	12.628	16.899
100	20.195	16.690
110	21.172	9.825
120	22.835	2.993

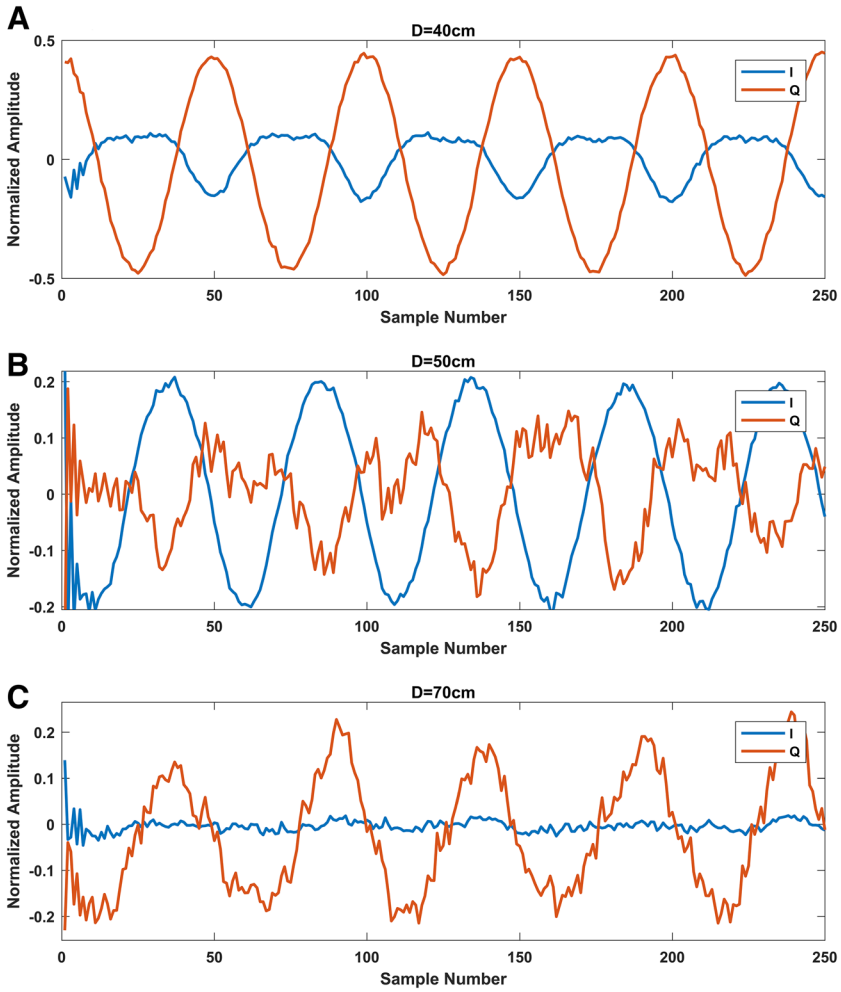

Fig. 5 Channels I and Q close to their null and optimum points. At distance D = 40 cm (**a**), both channels I and Q are away from their null point regions. At distance D = 50 cm (**b**), channel I approaches its optimum point, while channel Q approaches its null point. At distance D = 70 cm (**c**), channel Q approaches its optimum point, while channel I approaches its null point

3.1.2 Multi-tone measurements

The performance of the above proposed signal processing scheme, involving demodulation and MRA, was analyzed using multi-tone waveforms simulating chest wall movements. A_{1var}, representing respiration amplitude, was set to 3 mm and A_{2var}, representing heart rate amplitude, was maintained at 0.5 mm. Figure 6 illustrates the demodulated Doppler radar signal (Panel A) captured from a multi-tone waveform test bench setup with f_{1var} and f_{2var} set to 0.2334 and 1 Hz, respectively, to simulate a respiratory rate of 14 breaths per minute and a heart rate of 60 beats per minute. Figure 6 (Panels B and C) illustrates the isolation of respiratory and heart rate components from the demodulated signal using MRA. The mother wavelet employed for MRA was Symlet 10.

Table 2 shows the performance of the signal processing scheme in respiratory as well as heart rate reconstruction. During the first part of the measurements, heart rate and distance to test-bench were held constant at 55 beats per minute and 40 cm. The respiratory rate of the test-bench was varied from 6 to 24 breaths per minute in steps of 2. Similarly, during the second part of the measurements, respiratory rate was held constant at 14 breaths per minute at the same distance. The heart rate was varied from 45 to 95 beats per minute in steps of 5. The respiratory and heart rates were calculated, as breaths and beats per minute, using the product of the dominant frequency of the approximate and detail coefficients of 5th level MRA decomposition with the constant 60.

3.2 Volunteer study

3.2.1 Limb movements

Upon performing MRA on the demodulated signal, limb movements are isolated as the detail coefficients of 4th level decomposition (CD_4). Figure 7 illustrates a sample response of the polysomnography (Panel A) and that of the prototype (Panel B) to the limb movements of volunteer 2, measured over a period of 5 h. Double-epochs (60 s) were labeled (classified) to be containing limb movements if the

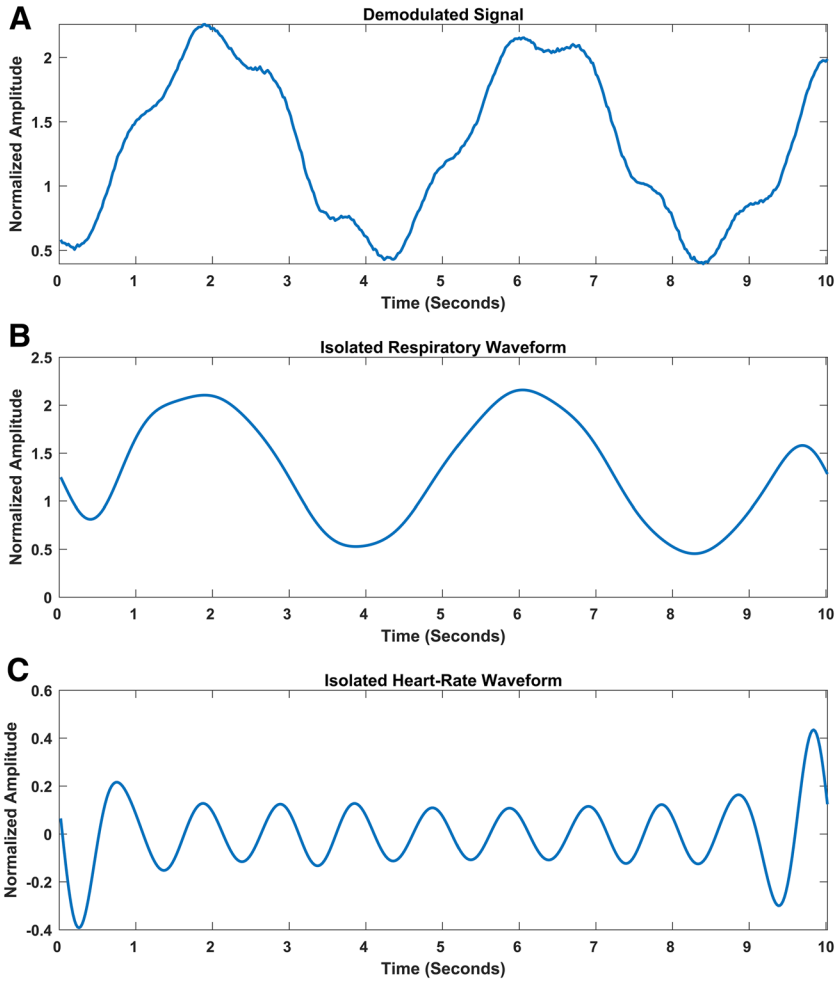

Fig. 6 **a** Sample multi-tone waveform with a respiratory rate of 14 breaths per minute and a heart rate of 60 beats per minute. **b** Extracted respiratory and **c** heart rate components

Table 2 Multi-tone simulation results for the scenarios of constant heart rate (HR) varying respiratory rate (RR) and constant RR and varying HR

Const. HR (55 BPM)			Const. RR (14 BrPM)		
Set_{RR}	Mea_{RR}	Er%	Set_{HR}	Mea_{HR}	Er%
6	6.00	0.00	45	45.00	0.00
8	7.85	−1.86	50	50.03	0.06
10	9.94	−0.63	55	55.01	0.02
12	12.12	0.98	60	59.99	−0.01
14	13.99	−0.06	65	65.02	0.03
16	16.08	0.49	70	70.00	0.00
18	18.02	0.13	75	75.03	0.04
20	20.06	0.31	80	80.01	0.02
22	22.05	0.25	85	84.99	−0.01
24	24.02	0.10	90	90.02	0.03
			95	95.00	0.00

BPM beats per minute, *BrPM* breaths per minute, Set_{RR} simulated respiratory rate, Set_{HR} simulated heart rate, Mea_{RR} measured respiratory rate, Mea_{HR} measured heart rate, and *Er%* relative percentage error

root-mean-square (RMS) value of its CD_4 exceeded a preset threshold. Upon synchronizing a total of 9-h data recordings from both the volunteers, 518 double-epochs were classified (movement = 1 and no-movement = 0) and the classification from the prototype was compared to that of the reference polysomnography to assess its sensitivity and specificity. The analysis has yielded the following results, shown in Table 3.

3.2.2 *Respiratory rate*

Upon identification and isolation of epochs with limb movements, using the above described classification scheme, the remaining epochs were processed to derive the respiratory and heart rates. 429 double-epochs (60 s) were used for respiratory rate statistical analysis, with the measurements ranging 14.6–22.0 breaths per minute. Double-epoch (60 s) analysis provided adequate resolution and resulted in minimal estimation error, hence was preferred over single-epoch (30 s) analysis for respiratory rate estimations. A moving average of window length 5 was used to smooth the respiratory rate estimates. Figure 8 shows the Bland–Altman

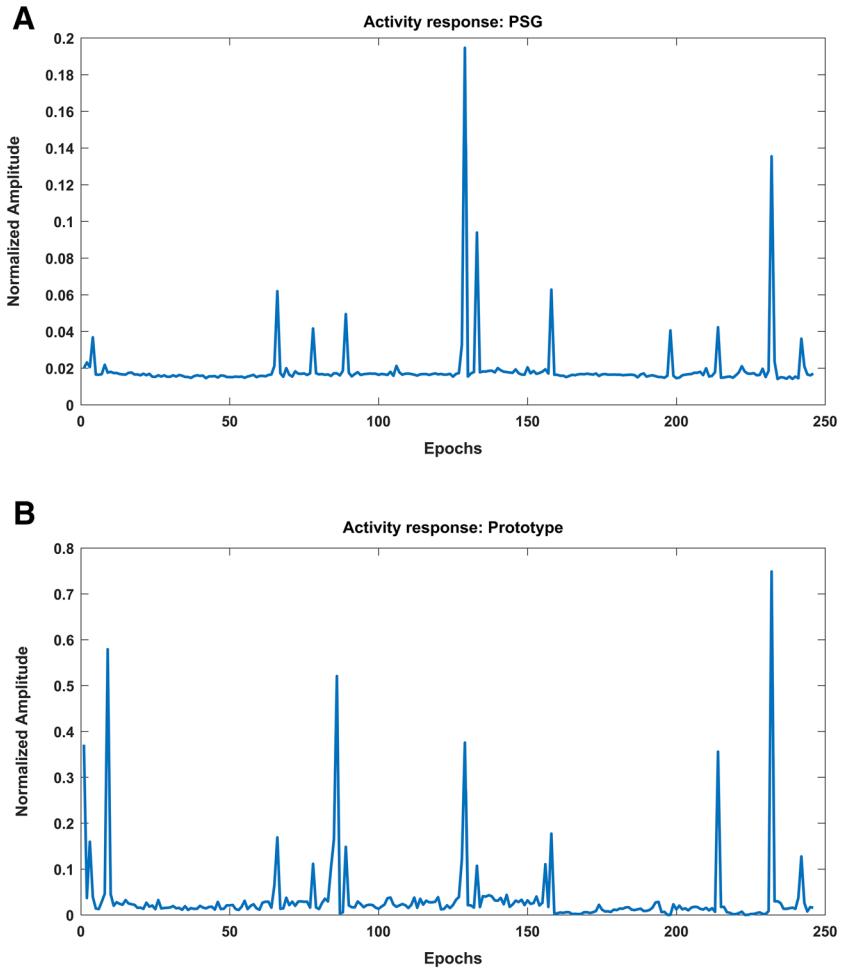

Fig. 7 Overnight activity response of the reference polysomnography (**a**) and that of the prototype mapped to the reference (**b**)

Table 3 Sensitivity–specificity analysis of limb movement classification

	Sensitivity (%)	Specificity (%)
Volunteer 1	81.97	71.79
Volunteer 2	95.75	81.82
	88.86	76.81

analysis for RR_{Prt} (prototype) and RR_{Ref} (polysomnography). The overall absolute error in respiratory rate estimate is within the range of 1 breath per minute.

3.2.3 Heart rate

Heart rate estimates pertaining to a single volunteer, from the reference polysomnography and the prototype, were used for carrying out statistical analysis. As heart rate has higher variability in comparison with the respiratory rate, epochs of 30-s length were used for deriving the heart rate estimates. Consequently, 446 such epochs were used for heart rate Bland–Altman analysis, with the measurements ranging

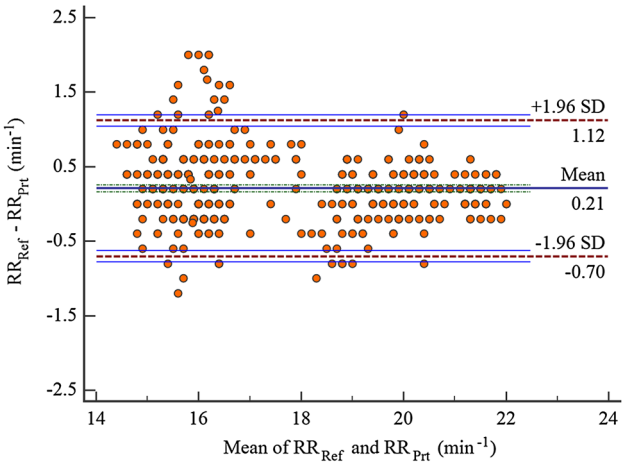

Fig. 8 Bland–Altman analysis for respiratory rate estimates from RR_{Prt} (prototype) and RR_{Ref} (polysomnography). *Solid black line* mean bias; *dotted red lines* lower and upper limits of agreement; *solid blue lines* 95% confidence intervals for *lower* and *upper limits* of agreement; *dotted green lines* 95% confidence interval for mean bias

54.9–65.1 beats per minute. Figure 9 shows the Bland–Altman analysis for HR_{Prt} (prototype) and HR_{Ref} (polysomnography). The overall absolute error in heart rate estimate is within the range of 3 beats per minute.

4 Discussion

This study successfully demonstrates the overall feasibility of K-band Doppler radar for contact-less overnight sleep marker measurements. We presented the development of a miniature setup for home-based long-term usage, using a 24 GHz Doppler transceiver, as well as its signal processing scheme, the Arc Tangent method for demodulation and the MRA for the reconstruction of physiological parameters. Single- and multi-tone test bench simulations showed extremely low relative percentage errors of the prototype for respiratory and heart rate within −2 and 1%. The volunteer setup demonstrated high agreement between the prototype and the gold standard polysomnography for the overnight assessment of limb movements, respiratory and heart rate.

Arc Tangent demodulation has been the preferred demodulation method in the literature and the same was employed in this study. Estimation of the static distance, existing as DC offsets in the I and Q channels, was a major challenge. Sole reliance on algebraic center estimation algorithms, such as the Taubin fit method, for DC offset tracking has resulted in erroneous estimates and demodulation. Similarly, iterative center estimation algorithms, such as Levenberg–Marquardt, failed to achieve accurate convergence when initialized with randomized initial conditions. The performance of center estimation and DC offset tracking has significantly improved when iterative algorithms were initialized with the results of algebraic fits as their initial conditions.

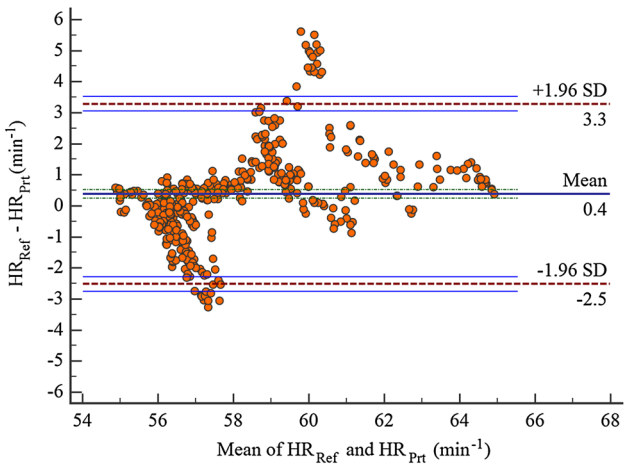

Fig. 9 Bland–Altman analysis for heart rate estimates form HR_{Prt} (prototype) and HR_{Ref} (polysomnography). *Solid black line* mean bias; *dotted red lines lower* and *upper limits* of agreement; *solid blue lines* 95% confidence intervals for *lower* and *upper limits* of agreement; *dotted green lines* 95% confidence interval for mean bias

Doppler radar undergoing wavelet transforms and MRA offers a good framework for the assessment of these physiological signals due to their well-defined frequency regions and non-stationary behavior. Although continuous wavelet transform offers a fine-grained frequency analysis, MRA using discrete wavelet transform was chosen due its dyadic down sampling. This enabled a signal decomposition scheme with its pre-defined levels spanning over the frequency ranges of the physiological signals of interest. Guided by the parameters of center frequency and the number of vanishing moments, we experimented with a range of wavelets found Symlet 10 as an optimal candidate.

The test bench setup simulating chest wall movements was very efficient and crucial to understand the response of the developed prototype. Single-tone simulations were pivotal in estimating radar channel imbalances and optimal operational distance. Distances in the range 20–30 cm offered a good SNR for both channels and resolved the null point problem. Such distances, however, might be obtrusive to the subject/patient due to voluntary limb movements during sleep with probable physical contact. A distance of 40 cm seems to be optimal with good SNR in both channels as well as with considerably lower probability of contact with the subject/patient during limb movements. With distances of 50 cm and above, the SNR of either or both the channels suffers due to increase in the background clutter. The results of multi-tone simulations using the test bench established the performance of the signal processing scheme involving demodulation and MRA. Precise reconstruction of respiratory and heart rate waveforms, from the demodulated signal, was feasible using MRA with relative errors below 1% in most cases.

Overnight volunteer studies have achieved satisfactory results that are in line with our test bench simulations. Our system has achieved an overall sensitivity of 88.86% and specificity of 76.81% in limb movement classification. The slightly lower specificity score can be attributed to the specificity of volunteer 1, who was awake and moving for a period of 1 h before falling asleep. Furthermore, we believe that a full-scale adequately powered volunteer study will be essential to accurately assess the sensitivity and specificity parameters of the prototype. The respiratory rate estimates from our prototype agree well with that of the reference polysomnography. The overall absolute error was one breath cycle per minute, which is well within the clinically acceptable range. Although complete overnight polysomnography was carried out for both the volunteers, the heart rate measurements from only one volunteer were used for statistical analysis as the reference heart rate recordings from the second volunteers were of low quality, possibly due to electrode displacements during sleep. Like the respiratory

rate estimates, heart rate estimates from our prototype agree well with that of the reference and lie within an overall absolute error range of 3 beats per minute.

Epochs (represented as circles) falling outside the limits of standard deviations in the Bland–Altman plots (Figs. 8, 9) for respiratory and heart rate estimates were further investigated. A majority of these outliers are the result of imprecise IQ center tracking, occurring immediately after the incidence of limb movements, causing erroneous demodulation, hence imprecise estimates. The peak detection scheme, used for the calculation of the respiratory rates, occasionally failed to mark in-complete peaks occurring at the extremes of an epoch, further resulting in outliers.

The results of our overnight volunteer studies are in-line with recently reported studies. Fox et al. [37] have compared, SleepMinder, a Doppler radar based biomotion sensor with a medical grade Actigraph and reported a sensitivity of 79% and specificity of 75%. Shouldice et al. [38] have compared SleepMinder derived respiratory rates with those from reference polysomnography and reported an overall error of 1 breath per minute. Rahman et al. [39] employed a similar K-band system and reported a mean absolute error of 3.29 and 1.98 cycles per minute for respiratory and heart rate estimations, respectively. Although overnight studies were performed, neither full-scale polysomnography, nor medical grade devices were used as reference methods in the later study. In their recent work, Hosseini et al. [40] also employed a K-band based system and achieved higher levels of accuracy (relative error less than 1.5%) for heart rate measurements by using an extensive model of the reflected signal.

This work has limitations. The multi-tonal simulations model respiratory movement of the chest wall as a single sine wave and do not include the effect of respiratory harmonics. A similar shortcoming exists with the heart rate simulation as well. Implementing mathematical models of higher order may improve simulations of the chest wall movement under the influence of periodic respiration and heartbeats. We envisage carrying out overnight polysomnographic studies involving more healthy volunteers to enable more accurate estimation of accuracy, precision, and reproducibility of the prototype.

5 Conclusion

K-band Doppler radar undergoing wavelet transforms and MRA is feasible and seems to be accurate for contact-less overnight sleep marker assessment. The validity of the system has to be confirmed in adequately powered volunteer and clinical studies. Further technological refinements of K-band Doppler radar might deliver robust performance in non-clinical and home-based settings. The novelty and advantage of this technology lies in simultaneous contact-less measurement of overnight limb movements, respiratory and heart rates using a single transceiver module. This is very much in contrast with the current home-based technologies that typically employ accelerometers/actigraphy for limb movements, respiratory inductance plethysmography (RIP) for respiratory rate measurement, and skin electrodes for heart rate measurement. As demonstrated in this pilot-study, Doppler radar technology can offer the very same physiological information with increased comfort and ease of operation. We plan to combine this contact-less physiological data acquisition system with a sleep classification framework to achieve home-based sleep monitoring, diagnosis and assessment.

Acknowledgements We thank Ms. Bühler and Ms. Morais, sleep technicians of Sleep-Wake-Epilepsy-Centre, Department of Neurology, Inselspital, Bern University Hospital, for their valuable support in performing overnight PSG recordings.

Funding This study was funded by departmental funding only.

Compliance with ethical standards

Conflict of interest The authors declare that they have no conflict of interest.

References

1. Gustavsson A, Svensson M, Jacobi F, Allgulander C, Alonso J, Beghi E, Dodel R, Ekman M, Faravelli C, Fratiglioni L, Gannon B, Jones DH, Jennum P, Jordanova A, Jonsson L, Karampampa K, Knapp M, Kobelt G, Kurth T, Lieb R, Linde M, Ljungcrantz C, Maercker A, Melin B, Moscarelli M, Musayev A, Norwood F, Preisig M, Pugliatti M, Rehm J, Salvador-Carulla L, Schlehofer B, Simon R, Steinhausen HC, Stovner LJ, Vallat JM, Van den Bergh P, van Os J, Vos P, Xu W, Wittchen HU, Jonsson B, Olesen J, Group CD. Cost of disorders of the brain in Europe 2010. Eur Neuropsychopharmacol. 2011;21(10):718–79. doi:10.1016/j.euroneuro.2011.08.008.
2. Ohayon MM. Epidemiology of insomnia: what we know and what we still need to learn. Sleep Med Rev. 2002;6(2):97–111.
3. Riemann D. Primary insomnia: a risk factor to develop depression? J Affect Disord. 2003;76(1–3):255–9. doi:10.1016/s0165-0327(02)00072-1.
4. Peppard PE, Young T, Barnet JH, Palta M, Hagen EW, Hla KM. Increased prevalence of sleep-disordered breathing in adults. Am J Epidemiol. 2013;177(9):1006–14. doi:10.1093/aje/kws342.
5. McNicholas WT, Bonsignore MR. Sleep apnoea as an independent risk factor for cardiovascular disease: current evidence, basic mechanisms and research priorities. Eur Respir J. 2006;29:156–78.
6. Lam EWK, Chung F, Wong J. Sleep-disordered breathing, postoperative delirium, and cognitive impairment. Anesth Analg. 2017;124(5):1626–35. doi:10.1213/ANE.0000000000001914.
7. Mathis J, Schreier D. Daytime sleepiness and driving behaviour (Tagesschlafrigkeit und Fahrverhalten.). Ther Umsch. 2014;71(11):679–86.

8. Ferrie JE, Kumari M, Salo P, Singh-Manoux A, Kivimäki M. Sleep epidemiology—a rapidly growing field. Int J Epidemiol. 2011;40(6):1431–7. doi:10.1093/ije/dyr203.
9. Flemons WW, Douglas NJ, Kuna ST, Rodenstein DO, Wheatley J. Access to diagnosis and treatment of patients with suspected sleep Apnea. Am J Respir Crit Care Med. 2004;169(6):668–72. doi:10.1164/rccm.200308-1124PP.
10. Benca RM. Diagnosis and treatment of chronic insomnia: a review. Psychiatr Serv. 2005;56(3):332–43. doi:10.1176/appi.ps.56.3.332.
11. Berry RB BR, Gamaldo CE, Harding SM, Lloyd RM, Marcus CL, Vaughn BV, The American Academy of Sleep Medicine. (2012) The AASM manual for the scoring of sleep and associated events: rules, terminology and technical specifications, Version 2.3.
12. Newell J, Mairesse O, Verbanck P, Neu D. Is a one-night stay in the lab really enough to conclude? First-night effect and night-to-night variability in polysomnographic recordings among different clinical population samples. Psychiatry Res. 2012;200(2–3):795–801. doi:10.1016/j.psychres.2012.07.045.
13. Meyer TJ, Eveloff SE, Kline LR, Millman RP. One negative polysomnogram does not exclude obstructive sleep apnea. Chest. 1993;103(3):756–60.
14. Levendowski DJ, Zack N, Rao S, Wong K, Gendreau M, Kranzler J, Zavora T, Westbrook PR. Assessment of the test–retest reliability of laboratory polysomnography. Sleep Breathing. 2009;13(2):163–7. doi:10.1007/s11325-008-0214-6.
15. Monk TH, Reynolds CF, Kupfer DJ, Buysse DJ, Coble PA, Hayes AJ, Machen MA, Petrie SR, Ritenour AM. The Pittsburgh sleep diary. J Sleep Res. 1994;3(2):111–20. doi:10.1111/j.1365-2869.1994.tb00114.x.
16. Frankel BL, Coursey RD, Buchbinder R, Snyder F. Recorded and reported sleep in chronic primary insomnia. Arch Gen Psychiatry. 1976;33(5):615–23. doi:10.1001/archpsyc.1976.01770050067011.
17. Harvey AG, Tang N. (Mis)Perception of sleep in insomnia: a puzzle and a resolution. Psychol Bull. 2012;138(1):77–101. doi:10.1037/a0025730.
18. Cole RJ, Kripke DF, Gruen W, Mullaney DJ, Gillin JC. Automatic sleep/wake identification from wrist activity. Sleep. 1992;15(5):461–9.
19. Pollak CP, Tryon WW, Nagaraja H, Dzwonczyk R. How accurately does wrist actigraphy identify the states of sleep and wakefulness? Sleep. 2001;24(8):957–65.
20. Snyder F, Hobson JA, Morrison DF, Goldfrank F. Changes in respiration, heart rate, and systolic blood pressure in human sleep. J Appl Physiol. 1964;19:417–22.
21. Stradling JR, Chadwick GA, Frew AJ. Changes in ventilation and its components in normal subjects during sleep. Thorax. 1985;40(5):364–70. doi:10.1136/thx.40.5.364.
22. Pedro F, Xi L, Mustafa R, Reinder H, Ronald MA, Jérôme R. Sleep stage classification with ECG and respiratory effort. Physiol Meas. 2015;36(10):2027.
23. De Chazal P, Sadr N Sleep apnoea classification using heart rate variability, ECG derived respiration and cardiopulmonary coupling parameters. In: 2016 38th Annual international conference of the IEEE Engineering in Medicine and Biology Society (EMBC), 16–20 Aug 2016. pp. 3203–3206. doi:10.1109/EMBC.2016.7591410.
24. Yavari E, Boric-Lubecke O, Yamada S. Radar principles. In: Doppler radar physiological sensing. Hoboken: Wiley; 2016. pp. 21–38. doi:10.1002/9781119078418.ch2.
25. Lin JC. Noninvasive microwave measurement of respiration. Proc IEEE. 1975;63(10):1530. doi:10.1109/PROC.1975.9992.
26. Wang J, Wang X, Chen L, Huangfu J, Li C, Ran L. Noncontact distance and amplitude-independent vibration measurement based on an extended DACM algorithm. IEEE Trans Instrum Meas. 2014;63(1):145–53. doi:10.1109/TIM.2013.2277530.
27. Park BK, Boric-Lubecke O, Lubecke VM. Arctangent demodulation with DC offset compensation in quadrature Doppler radar receiver systems. IEEE Trans Microw Theory Tech. 2007;55(5):1073–9. doi:10.1109/TMTT.2007.895653.
28. Lin HD, Lee YS, Chuang BN. Using dual-antenna nanosecond pulse near-field sensing technology for non-contact and continuous blood pressure measurement. In: 2012 Annual International Conference of the IEEE engineering in Medicine and Biology Society, 28 Aug 2012–1 Sept 2012. pp. 219–22. doi:10.1109/EMBC.2012.6345909.
29. Byung-Kwon P, Yamada S, Boric-Lubecke O, Lubecke V. Single-channel receiver limitations in Doppler radar measurements of periodic motion. In: 2006 IEEE Radio and Wireless Symposium, 17–19 Jan 2006. pp. 99–102. doi:10.1109/RWS.2006.1615104.
30. Xu W, Gu C, Li C, Sarrafzadeh M. Robust Doppler radar demodulation via compressed sensing. Electron Lett. 2012;48(22):1428–30.
31. Zakrzewski M, Raittinen H, Vanhala J. Comparison of center estimation algorithms for heart and respiration monitoring with microwave Doppler radar. IEEE Sens J. 2012;12(3):627–34. doi:10.1109/JSEN.2011.2119299.
32. Boric-Lubecke O, Lubecke V, Mostafanezhad I. Amplitude modulation issues in Doppler radar heart signal extraction. In: 2011 IEEE topical conference on biomedical wireless technologies, networks, and sensing systems. 2011. doi:10.1109/BIOWIRELESS.2011.5724357.
33. Bentley PM, McDonnell JTE. Wavelet transforms: an introduction. Electron Commun Eng J. 1994;6(4):175–86. doi:10.1049/ecej:19940401.
34. Mallat SG. A theory for multiresolution signal decomposition: the wavelet representation. IEEE Trans Pattern Anal Mach Intell. 1989;11(7):674–93. doi:10.1109/34.192463.
35. Martin Bland J, Altman D. Statistical methods for assessing agreement between two methods of clinical measurement. Lancet. 1986;327(8476):307–10. doi:10.1016/S0140-6736(86)90837-8.
36. Bland JM, Altman DG. Measuring agreement in method comparison studies. Stat Methods Med Res. 1999;8(2):135–60. doi:10.1177/096228029900800204.
37. Fox NA, Heneghan C, Gonzalez M, Shouldice RB, De Chazal P. An evaluation of a non-contact biomotion sensor with actimetry. In: 2007 29th Annual International Conference of the IEEE Engineering in Medicine and Biology Society. doi:10.1109/IEMBS.2007.4352877.
38. Shouldice RB, Heneghan C, Petres G, Zaffaroni A, Boyle P, McNicholas W. Chazal Pd Real time breathing rate estimation from a non contact biosensor. In: 2010 Annual International Conference of the IEEE Engineering in Medicine and Biology, 31 Aug 2010–4 Sept 2010. pp. 630–3. doi:10.1109/IEMBS.2010.5627275.
39. Rahman T, Adams AT, Ravichandran RV, Zhang M, Patel SN, Kientz JA, Choudhury T. (2015) DoppleSleep: a contactless unobtrusive sleep sensing system using short-range Doppler radar. Paper presented at the Proceedings of the 2015 ACM International Joint Conference on Pervasive and Ubiquitous Computing, Osaka, Japan.
40. Hosseini SMAT, Amindavar H. A new Ka-band Doppler radar in robust and precise cardiopulmonary remote sensing. IEEE Trans Instrum Meas. 2017. doi:10.1109/TIM.2017.2714480.